Journal of
Composites Science

MDPI

Article

A Design Optimization Study of Step/Scarf Composite Panel Repairs, Targeting the Maximum Strength and the Minimization of Material Removal

Spyridon Psarras *, Maria-Panagiota Giannoutsou and Vassilis Kostopoulos

Laboratory of Applied Mechanics, Mechanical Engineering and Aeronautics Department, University of Patras, Greece University Campus, 26504 Rio Achaia, Greece
* Correspondence: spsarras@upatras.gr

Abstract: This study aimed to optimize the geometry of composite stepped repair patches, using a parametric algorithm to automate the process due to the complexity of the optimization problem and various factors affecting efficiency. More specifically, the algorithm initially calculates the equivalent strengths of the repaired laminate plate according to a max stress criterion, then calculates the dimensions of several elliptical repair patches, taking into account several design methods extracted from the literature. Next, it creates their finite element models and finally, the code conducts an assessment of the examined patch geometries, given specific user-defined criteria. In the end, the algorithm reaches a conclusion about the optimum patch among the designed ones. The algorithm has the potential to run for many different patch geometries. In the current research, five patch geometries were designed and modeled under uniaxial compressive loading at 0°, 45° and 90°. Overall, the code greatly facilitated the design and optimization process and constitutes a useful tool for future research. The results revealed that elliptical stepped patches can offer a near-optimum solution much more efficient than that of the conservative option of the circular patch, in terms of both strength and volume of healthy removed material.

Keywords: repair patch optimization; elliptical geometry; parametric study; algorithm

Citation: Psarras, S.; Giannoutsou, M.-P.; Kostopoulos, V. A Design Optimization Study of Step/Scarf Composite Panel Repairs, Targeting the Maximum Strength and the Minimization of Material Removal. *J. Compos. Sci.* **2024**, *8*, 248. https://doi.org/10.3390/jcs8070248

Academic Editor: Francesco Tornabene

Received: 22 May 2024
Revised: 16 June 2024
Accepted: 20 June 2024
Published: 30 June 2024

1. Introduction

The repair of composite structures constitutes a directly applicable and cost-effective solution for the extension of a structure's service life. According to Federal Aviation Administration Order 8900,1A [1], all critical structures will have an additional repair size limit to be no larger than a size that retains limit load (ultimate residual strength) capability with the failed repair within the constraints of arresting design features (in the repair or base structure). For the purposes of stress analysis and repair certification, the machined surface, rather than the original defect, should be taken into account. If the machined area is too large, the repair must be bolted or thrown away. As a result, enhancing stress analysis and repair geometries will minimize the machined surface and increase the repairability of composite structures, especially for repairs that involve adhesively bonding a composite repair patch into a suitably formed cavity with the same geometry as the patch. The reason for stepped and scarf patches' popularity is the fact that they offer a flat final surface to the repaired structure, in this way satisfying aerodynamic and hydrodynamic requirements. Furthermore, they provide a smooth and uniform load transfer from the repaired structure to the patch, as the adhesive bonding area provides a large load transfer surface, contrary to mechanical connections, like the ones that include rivets. Additionally, the adhesive "seals" the connection and often protects it from humidity-caused damage. Another crucial advantage of adhesively bonded repairs is the absence of holes for screw or bolt implementation, which prevents stress concentration at connection points that could

degrade the structure. Finally, as reported in the literature, adhesive repairs exhibit a high strength and fatigue life, as well as slower crack propagation [2–6].

In composite materials, the fibers are aligned in specific directions and an elliptical patch can align better with these fibers; the elliptical repair patches are the favored option due to their superior balance of stress distribution, aerodynamic efficiency and structural integration [7–9]. Because of their design, the forces may be distributed more evenly and smoothly, preserving the integrity and functionality of the repaired structure. However, the design and evaluation of different composite repair patches, for the purpose of forming an optimum patch design, is a complex and time-consuming process [10,11]. The geometry and effectiveness of a repair patch depend on various parameters, the most primary of which are briefly presented below.

To start with, the shape and the overall geometric morphology of the repair patch are crucial factors for determining how effective and applicable the repair is. The simplest choice of a repair patch that fits into a properly shaped cavity of a damaged structure is the circular-conical one. This approach has proven suitable for pseudo-isotropic plates that can have equal strength in all directions [5,12,13]. However, this choice seems quite conservative for structures made of composite materials, which are loaded in various directions, due to the changing stiffness within their volume and due to the fact that they have flexibility in their design. Because of these characteristics of composite materials, the circular patch might result in the removal of more healthy material than what is necessary to achieve the desired strength. In the effort to optimize the shape of repair patches, various hybrid shapes have been developed, which essentially combine elliptical and other flat shapes. Thus, several studies [12,14–18] have so far been aimed at the optimization of a repair patch's shape as regards both strength and the amount of pristine material removal, and patches of elliptical shapes seem to be much more sustainable.

The scarf angle is one of the most important parameters of a stepped/scarf repair, as it affects both the volume of the undamaged material that is removed to form the cavity in the parent structure and the final strength of the repair. It is worth noting that the sensitivity of the maximum stress values to changes in the scarf angle is significant (in study [5], an increase of up to 232% in maximum normal stresses was found for a scarf angle of 12° compared to a scarf angle of 3°). Generally, reducing the scarf angle leads to a decrease in stress concentration and a higher strength, but it also increases the size of the patch and, as a consequence, the volume of the removed material, which is undesirable. Therefore, a detailed investigation is necessary for the selection of the optimum scarf angle, so that a balance is guaranteed between the aforementioned controversial effects of the scarf angle on the repair and so that the possible geometric limitations of the overall repair are not exceeded. Except for the scarf angle, the term scarf ratio is also used to design and examine stepped or scarf repaired patches. The scarf ratio is defined as the ratio of the patch thickness to its maximum radius and it is thus equal to the tangent of the scarf angle:

$$scarf\ ratio = \frac{patch\ thickness}{patch's maximum\ radius} = \tan(scarf\ angle) \quad (1)$$

It is evident that the way the scarf ratio influences the behavior of the repair will be proportional to the effect of the scarf angle. Specifically, for high values of the scarf ratio, an increase in normal stresses and a decrease in the strength of the repair have been observed, while, conversely, for smaller scarf ratios, the strength increases as the load transfer area between the patch and the remaining structure increase, and the load distribution is more effective [19–21].

Furthermore, layup of both the parent structure and the patch may also have an influence on the repair's efficiency. A patch's layup might be in such a way that the fiber orientation of each layer of the patch either precisely aligns with the fiber orientation of the corresponding layer of the repaired structure or deviates by a certain degree. In the research conducted so far, neither of the two solutions has been proven as optimum, but it is common for the patch's layup to match the plate's layup [5,22]. In addition, although the

layer sequence affects the repair efficiency, the symmetry or asymmetry of the layup does not seem to have a significant impact on the amount of pristine removed material. Also, a common and expected conclusion from all the studies is that the stress concentration is located in the layers with a 0 degree fiber orientation. In fact, the maximum stresses increase when the 0 degree plies are near the ends of the joint. Lastly, it has been observed that the smaller the distance between the 0 degree layers, the lower the maximum shear stress values, as the load distributes among more stiff layers.

Additionally, the number of steps seems to influence the stress distribution, stress concentration, strength of the repair, as well as its damage tolerance [20,21]. Typically, one step corresponds to each layer and, in general, the results depend on the interaction of the number of steps with the layup. Therefore, specialized investigations are recommended regarding this problem.

The adhesive used between the repair patch and the repaired structure also affects the behavior of the repair. More specifically, by using an adhesive with a linear elastic behavior, stress concentrations are observed in the scarf joint as well as the stepped joint. In fact, adhesives used in repairs of mechanical structures exhibit a plastic behavior when temperature increases. This plasticity has proven beneficial for the bond's strength and damage tolerance, as stress concentrations near the 0 degree layers are relieved and stress distribution becomes more uniform [2,6]. Regarding the adhesive film thickness, according to the literature, thinner adhesive layers are more efficient, since they result in lower maximum normal and shear stresses. On the other hand, as adhesive thickness increases, deformations in the film are smaller. Consequently, it is recommended that the adhesive thickness is in the range from 0.125 to 0.25 mm.

Taking all the above into consideration and based on the authors' previous work [18,23,24], in the present study, an effort was made to develop a uniform and more automated parametric process of elliptical patch geometry design, finite element model construction and evaluation and comparison of the obtained results. An algorithm in Python was developed in the Abaqus PDE environment. The operations of the code, its inputs and its outputs are explained in the next paragraphs.

2. Materials and Methods

2.1. Materials

The calculations were conducted regarding a laminate plate with the following layup: $[45°/-45°/90°/0°/90°/0°/90°/-45°/45°]$. The patches' layup is the same as the 6 upper plies of the plate, as follows: $[0°/90°/0°/90°/-45°/45°]$. For both the plate and the patch composite material, Graphite/Epoxy UD IMS 24K 977-2 is considered. The hole representing the damage is 5 mm in diameter. The composite material properties that were used in the current study are presented in Tables 1–3.

Table 1. Elastic properties of the composite material applied to the code.

Elastic Properties		
Lamina Properties	**Symbol and Unit of Measure**	**Value**
Density	ρ [kg/mm^3]	1.597×10^{-6}
Elastic modulus—direction 1 (parallel to fibers)	E1 [MPa]	125,000
Elastic modulus—direction 2 (vertical to fibers)	E2 [MPa]	8680
Shear modulus—plane 12 (lamina plane)	G12 [MPa]	4700
Shear modulus—plane 23 (vertical to lamina plane)	G23 [MPa]	4700
Shear modulus—plane 13 (vertical to lamina plane)	G13 [MPa]	4700
Poisson's ratio—plane 12	v12	0.35

Table 2. Damage initiation properties of the composite material applied at the code.

Damage Initiation Properties		
Lamina Strengths	**Symbol and Unit of Measure**	**Value**
Tensile strength—direction 1 (parallel to fibers)	F1T [MPa]	3325
Compressive strength—direction 1 (parallel to fibers)	F1C [MPa]	911
Tensile strength—direction 2 (vertical to fibers)	F2T [MPa]	66
Compressive strength—direction 2 (vertical to fibers)	F2C [MPa]	170
Shear strength—lamina plane	S [MPa]	90
Shear strength—plane vertical to lamina plane	R [MPa]	60

Table 3. Damage evolution properties of the composite material applied at the code.

Damage Evolution Properties		
Lamina Strengths	**Symbol and Unit of Measure**	**Value**
Tensile fracture energy—direction 1 (parallel to fibers)	G_{FT}^{C} [N/mm]	163
Compressive fracture energy—direction 1 (parallel to fibers)	G_{FC}^{C} [N/mm]	70
Tensile fracture energy—direction 2 (vertical to fibers)	G_{MT}^{C} [N/mm]	0.5
Compressive fracture energy—direction 2 (vertical to fibers)	G_{MC}^{C} [N/mm]	17

The adhesive properties introduced to the model are experimentally validated in [14] and are presented below in Table 4.

Table 4. Adhesive properties applied to the code.

Adhesive Properties	**Symbol and Unit of Measure**	**Value**
Elastic Properties		
Stiffness modulus—normal direction	Kn [N/mm^3]	100
Stiffness modulus—first shear direction	Ks [N/mm^3]	35
Stiffness modulus—second shear direction	Kt [N/mm^3]	35
Damage initiation properties		
Strength—normal direction	t_n [MPa]	14
Strength—first shear direction	t_s [MPa]	40
Strength—second shear direction	t_t [MPa]	40
Damage evolution properties		
Critical fracture energy—normal direction	G_{IC} [N/mm^2]	400
Critical fracture energy—first shear direction	G_{IIC} [N/mm^2]	600
Critical fracture energy—second shear direction	G_{IIIC} [N/mm^2]	600

2.2. Methodology of the Study—The Algorithm

As mentioned previously, an algorithm was constructed to automate the process of designing, modeling and assessing the stepped elliptical patches (Figure 1). The algorithm consists of four main parts and its form is parametric to a great extent. After the explanation of the code's structure and operations, its application in the current study's problem and the required inputs are presented. In the first part of the algorithm, the equivalent compressive strengths of the composite plate in the x and y directions are calculated, taking into consideration the max stress criterion. In the second part, the user-defined inputs and the plate's strengths are used for the calculation of the stepped elliptical patches' dimensions. In the next part of the code, finite element models of a repaired plate with a patch are created in Abaqus. From past studies [18,23,24], the dimensions of the optimum circular patch regarding the laminate plate of the present study are known. Thus, each one of the designed elliptical repair geometries, as well as the optimum circular patch,

is modeled under the user-defined load types on user-defined load directions. Finally, a post-processing code extracts and analyzes the results of the analyses. In the present study, for comparison reasons, the term of r ratio is defined and used. The r ratio is, in fact, the ratio of strength per unit of undamaged removed material volume. This ratio is useful since it provides a measure of comparison between the strength of the repair and the volume of pristine material removal. This information is essential in order to reject patches that are very strong but also very big, because, in this case, a lot of pristine material would have to be removed from the repaired structure.

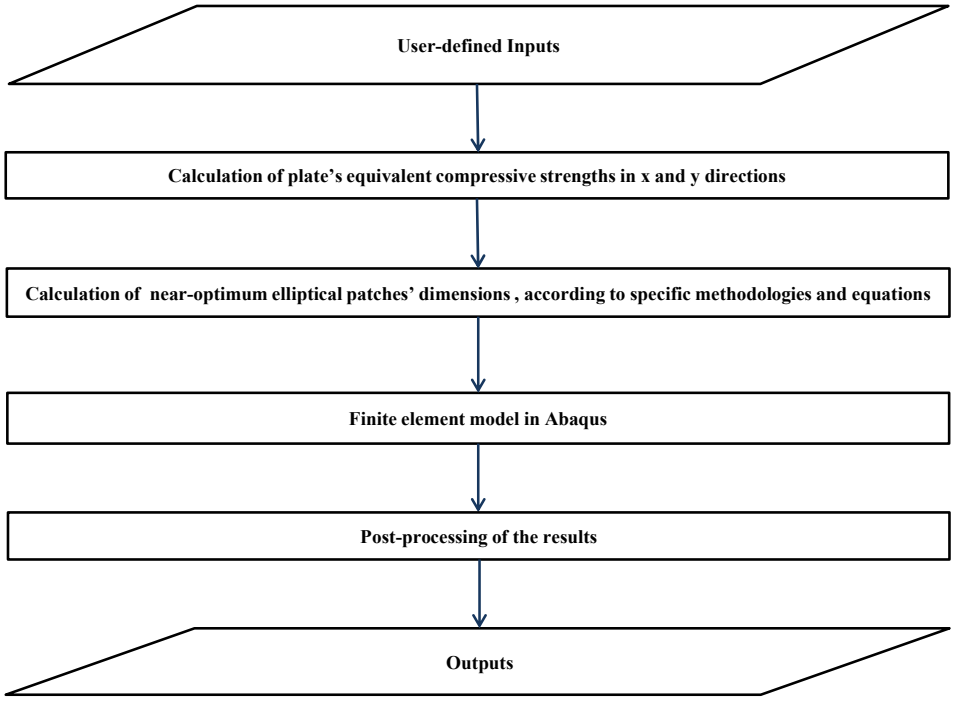

Figure 1. Flowchart of the algorithm's main operations.

The algorithm requires a set of input data in order to provide the desired results. Firstly, the layups of the damaged plate and the repair patch constitute the necessary input information. The layups are declared in the form of lists that are of a size that is the same as the number of plies of each structural compartment. Each element of the list is the value of the angle (in degrees) of the current ply orientation. Also, ply thickness, the composite materials' properties, the properties and thickness of the adhesive layer and the lamina's theoretical strengths (on the principal system) are defined. Additionally, coded names, according to the design fields, of the near-optimum elliptical patches are inserted in the code. The basic geometric characteristics of the parts are also necessary, such as the dimensions of the damaged plate, of the clamps and of the anti-buckling rods and the diameter of the circular blind hole that represents the damage in the plate. The relative distances between the parts in the model are declared by the user, too. Moreover, the load types and load directions under which the strength of the repair is examined are given in the form of lists. Finally, the user has to define the percentage of the allowable deviation of the near-optimum patch's strength and r ratio from the optimum circular patch's strength and r ratio, correspondingly.

All elliptical patches that were designed, regardless of the design methodology, have the same geometric features, as follows:

- Stepped.
- Every step's height is equal to one ply's thickness, so that each step corresponds to one ply.

- For each ply of the patch, the fiber direction has the same direction as the corresponding ply of the parent structure (patch and plate fiber direction coincide in each step)
- Elliptical form for each ply: from the bottom of the patch to its top, each ellipse is bigger than the previous one. Each smaller ellipse is fully inside the next one.

Each one of the repair patches was designed based on the following four fields: the orientation of each ply's ellipse, the type of load under which the repair is designed to exhibit sufficient strength, the method of the scarf angle's calculation and the method of the step length's calculation. For each field, alternative methodologies were implemented. Each patch is given a coded name regarding the design methods that are followed to calculate its dimensions. These methodologies are explained below.

Orientation of patch's ellipses: This field concerns the general arrangement of the ellipses that constitute the patch. More specifically, two different cases can be designed and a typical patch morphology of each case is shown in Figure 2. (a) Ellipses of all plies are parallel to the x direction and the code name for this design method is ***NR***. (b) The ellipse of each ply has a major axis parallel to the ply's fibers and the code name for this design method is ***R***.

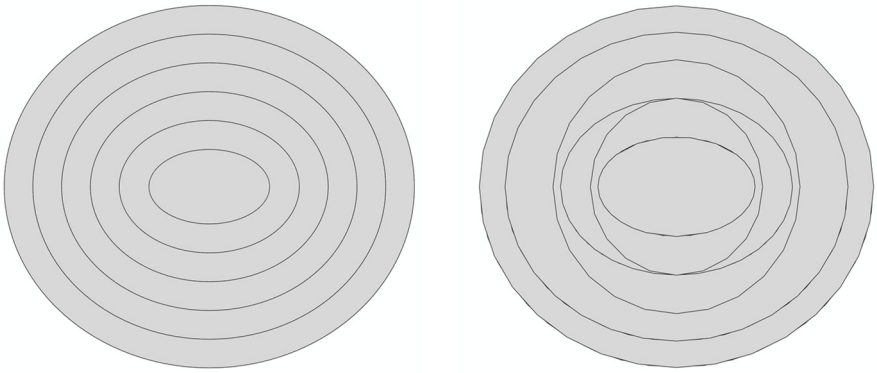

Figure 2. Example of patch (**a**) with the ellipses of all plies parallel to the fibers of 0° and (**b**) where the ellipse of each ply has its major axis parallel to the fibers of the current ply.

Design loads: Afterwards, the dimensions of the patch were calculated for the patch to exhibit sufficient strength under a specific load condition. Three theoretical ultimate load cases were considered, as follows:

- Uniaxial loading of plate under the plate's equivalent theoretical strength (x direction)—Coded name for this design method: ***XP***
- Biaxial loading of plate under the plate's equivalent theoretical strengths (x and y direction)—Coded name for this design method: ***XYP***
- Biaxial loading of each lamina under the lamina's strengths (principal system of lamina)—Coded name for this design method: ***12L***

Scarf angle calculation methods: The design methodologies of the scarf angle and step length were proposed in the literature for the design of stepped and scarf circular repair patches or simple 2D joints. These equations were suitably adapted to calculate the minor and major axis of the patches' ellipses.

- Max stress method [6]:

$$\theta = \frac{1}{2} \cdot sin\left(\frac{2 \cdot \tau f}{\sigma}\right) \quad (2)$$

θ: scarf angle
σ: stress on scarf angle's direction
τf: adhesive shear strength

The coded name for this design method is MS

- Max stress method, taking into consideration stress intensity factor K*t* [6]:

$$scarf\ angle = 0.5 \cdot \sin^{-1}\left(\frac{2 \times \tau f}{\mathrm{K}t \times \sigma}\right) \quad (3)$$

K_t stress concentration factor:

$$\mathrm{K}_t = \frac{n_{total}}{n_0 + n_{\pm 45}\frac{E_{45}}{E_0} + n_{90}\frac{E_{90}}{E_0}} \quad (4)$$

The coded name for this design method is KT

- Scarf angle is not calculated: a specific value is defined by the designer.

The coded name for this design method is ***NC***

Step calculation methods: Similarly to the equations for the calculation of scarf angle, the step calculation methods are proposed in the literature for the purpose of designing circular patches or 2D joints, and they were used in the present study for the calculation of the step length in the direction of the major and minor axis of each ply's ellipse.

- According to adhesive shear strength:

$$step = \frac{tp \times \sigma}{\tau f} \quad (5)$$

tp : thickness of the ply
τf : adhesive shear strength
σ : stress on the direction of the step

Coded name for this design method: ***AD***

- Fiber-oriented methodology [3]:

$$step = \frac{tp \times cos\beta}{tan(\theta min)} \quad (6)$$

Coded name for this design method: ***FD***

- According to geometry of the stepped profile:

$$step = \frac{tp}{tan\theta} \quad (7)$$

Coded name for this design method: ***G***

2.3. Concept of the Design Methodology

The calculation of an elliptical patch's dimensions is conducted ply-to-ply, beginning from the bottom ply of the patch. Next, for each ply, the calculations take place in the direction of the current ellipse's minor axis and then for the ellipse's major axis. Thus, initially, the smallest ellipse of the bottom ply of the patch is designed. The first ellipse's minor axis is always equal to the diameter of the hole that represents the damage, so that the least amount of material removal occurs for the first ply. Following, the first ellipse's major axis is calculated as follows: a method for scarf angle calculation is chosen and with the calculated angle known, a method for the step length is chosen. The next ellipse is designed similarly; however, it takes into consideration the geometric restrictions explained in the previous paragraph.

Every patch takes a coded name according to the design methods used, in the following form: Orientation of the ellipses—Design load—Scarf angle calculation method—Step calculation method.

2.3.1. First Part of the Algorithm: Calculation of Plate's Equivalent Strengths

The initial part of the code calculates the composite plate's theoretical equivalent strengths regarding the desired load types and load directions, as indicated using the max-stress criterion. The flowchart in Figure 3 shows the user-defined inputs that are used in this phase and the procedure of the calculations via nested loops.

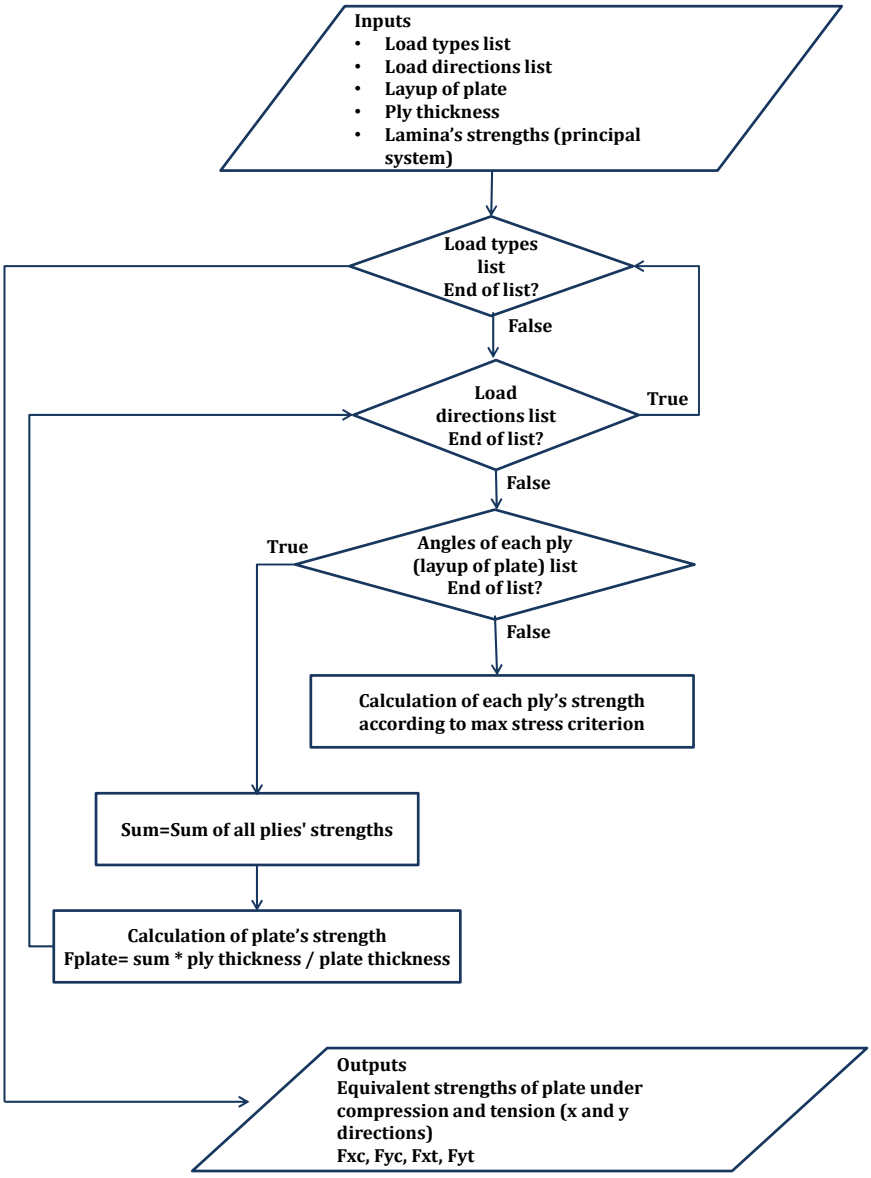

Figure 3. Flowchart of the first part of the code where the plate's equivalent strengths are calculated.

2.3.2. Second Part of the Algorithm: Patch Design

The second part of the algorithm constitutes the design part. The desired load types and load directions are introduced by the user as lists or arrays. For example, each element of the load direction array is a number that represents the angle of load direction in degrees. Coded names of repair patch designs are also introduced as inputs. A 'for loop' is used until all given patch names are iterated. After each iteration is completed, the dimensions of an elliptical patch are calculated.

First, considering the suitable stress situation, the stresses on the minor and major axis of each ply's ellipse are defined through a function. Then, another function is called to calculate the values of the scarf angle. Using the scarf angle values as inputs, the step length function is used to determine the length of the step in the corresponding directions. Finally, the lengths of the major and minor axis for each ply of the patch are calculated and saved. Furthermore, the same function calculates the volume of material loss, which the specific repair patch causes by its implementation on a structure with a hole that represents the damage. In the end of this part of the algorithm, the dimension of all near-optimum patches is saved. Figure 4 represents this procedure.

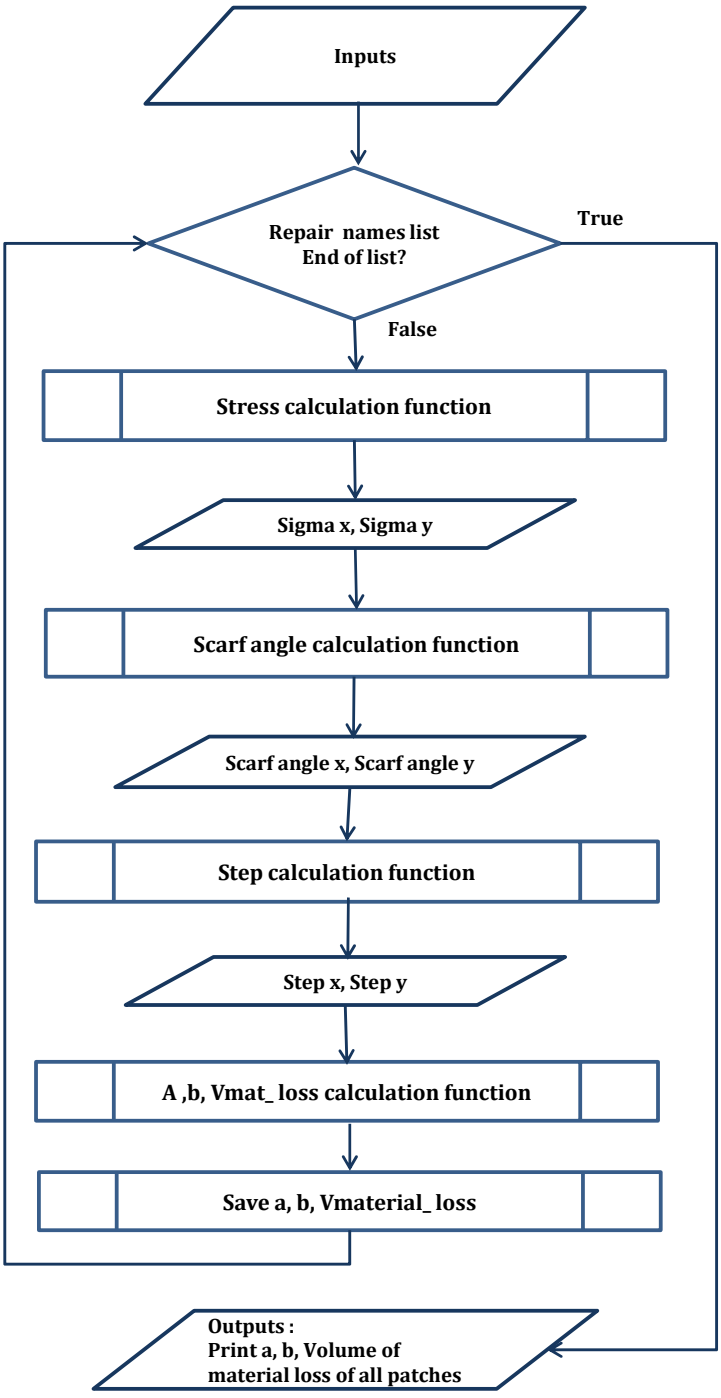

Figure 4. Flowchart of the second part of the code where the dimensions of elliptical patches and the corresponding volume of pristine material loss are calculated.

2.3.3. Third Part of the Algorithm: FE Model in Abaqus—The Code of Modeling

In this phase of the algorithm, each one of the elliptical repair geometries, as well as the optimum circular patch are modeled under the given load types and on the given directions. The code that creates the finite element model is in the form of a function that is suitably called within nested loops, as shown in Figure 5.

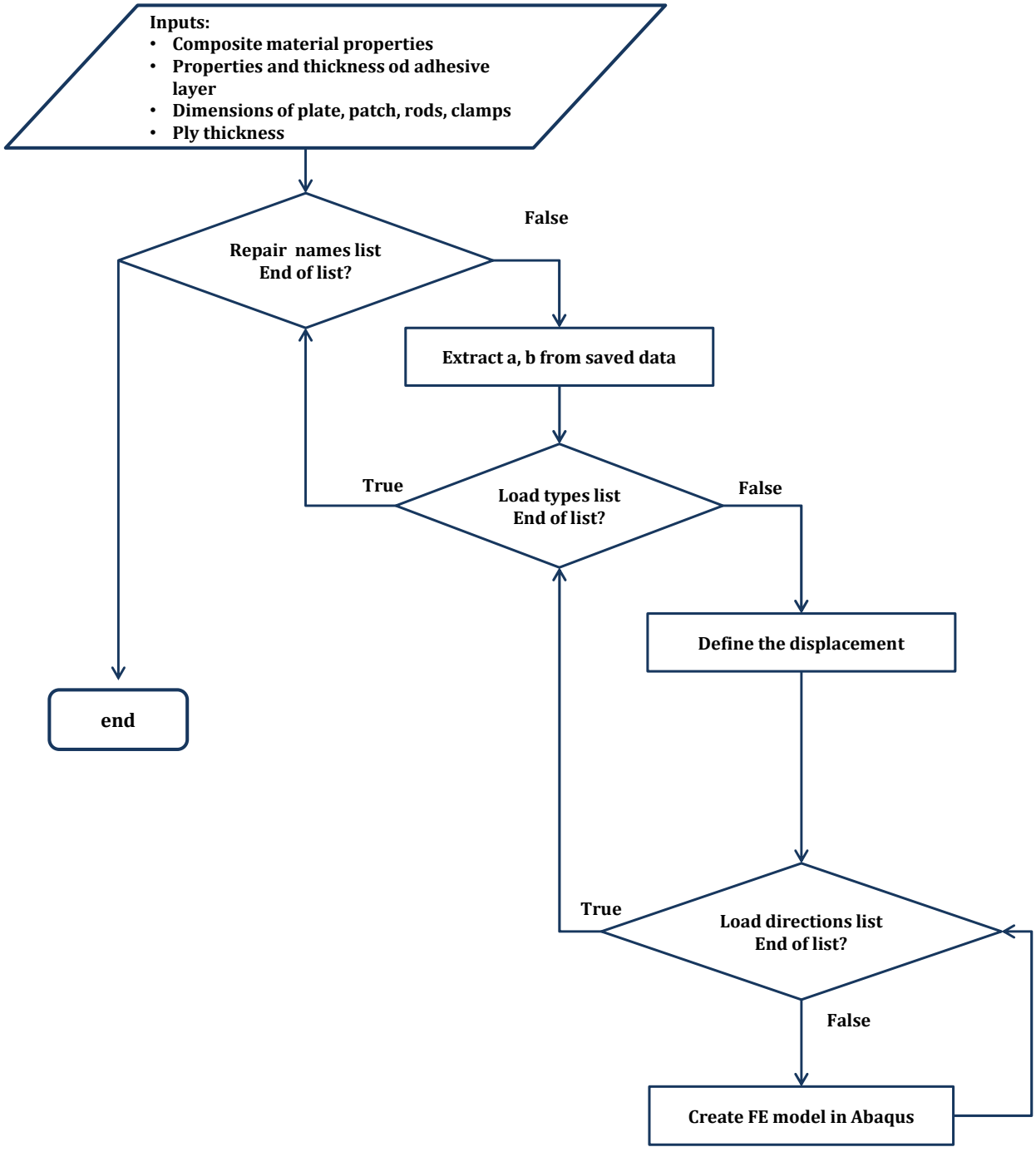

Figure 5. Flowchart of the third part of the code where the finite element models of the designed patches on the plate are created.

For every patch geometry, the calculated and saved data from the initial design part of the code are used by the algorithm to create the parts' geometries in Abaqus. Then, for every load type and every load direction, an FE model of the repaired plate with the current patch is created and analyzed. The procedure stops when all given patches are modeled under all given load conditions.

The designed repair patches are tested by implementing them on a laminate plate. All FE models that are created and analyzed in Abaqus are based on the same laminate plate. The configuration of the models is a simplified form of the experimental configuration, which is indicated by Airbus Standard AITM 1-0010 [25] for the purpose of determining the compressive strength of a laminate plate after an impact (Compression After Impact). More specifically, as in Figure 6, the plate is connected with two rigid clamps, one on each side surface. One of the two clamps has all its degrees of freedom restricted, and displacement is applied on the other clamp. Also, in order to avoid the possible buckling phenomena, the model features four anti-buckling, semi-tubular rods on the bottom surface of the plate, as well as four rods on the upper surface of the plate.

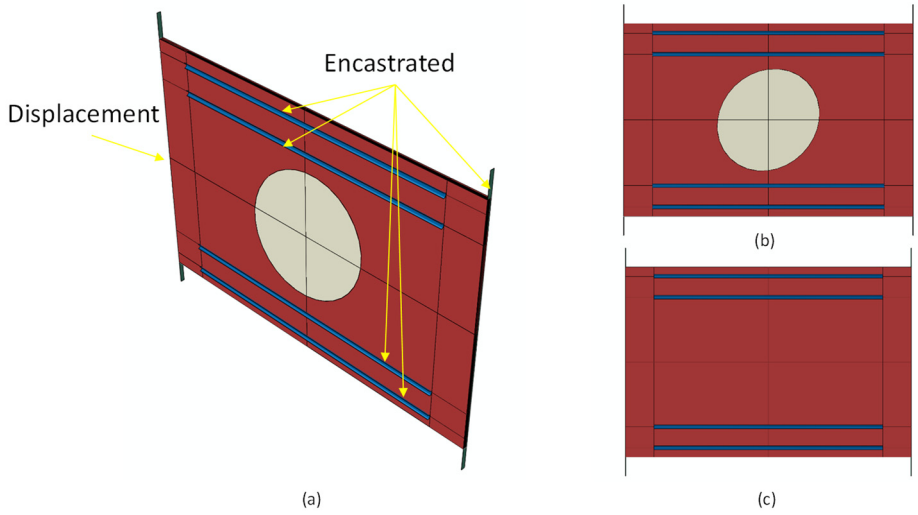

Figure 6. Example of (**a**) the repaired plate model with a near-optimum elliptical patch. On the left, the two sides of the plate; (**b**) repaired side and (**c**) back side.

After a convergence study, it was concluded that finite elements with edges of 1 mm in length are the most efficient for the plate and the patch, since this size provides sufficient discretization of the elliptical geometries and vital computational cost. Continuum shell, mainly hexahedral, elements were used for the plate and the patch, and quadrilateral elements were used for the rigid bodies (clamps and rods).

2.3.4. Fourth Part of the Algorithm

Finally, a post-processing code extracts and analyzes the results of the analyses (Figure 7). For each model, max force is extracted, and the ratio of strength per unit of undamaged removed material volume (r) is calculated. Also, the deviation [%] of r ratios and max forces from the corresponding values of the optimum circular repair are calculated, Figure 8. In the end, the patch that exhibits the maximum average r ratio (considering all load types) and does not offer an extreme low value of r or strength in any case is picked as optimum.

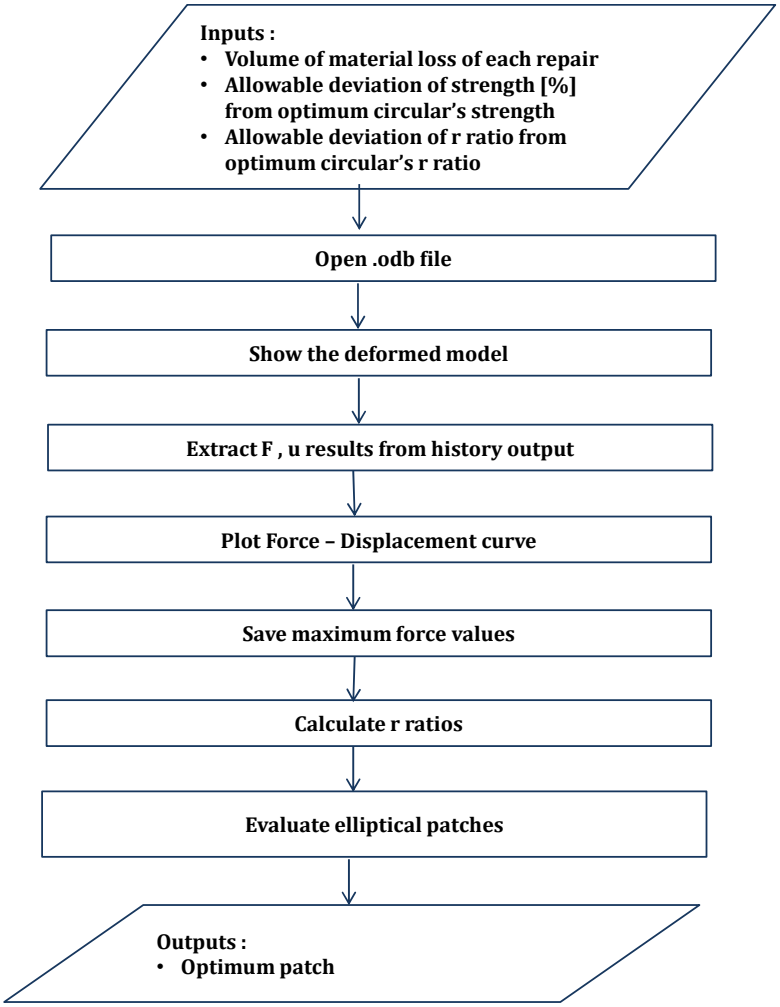

Figure 7. Flowchart of the fourth part of the code where the post-processing of the results takes place.

2.4. Parametric Characteristics of the Algorithm

As mentioned above, achieving an automated patch design and simulation procedure was the main goal of the algorithm. As a result, the code has some features that contribute to this purpose. The algorithm runs for any number of near-optimum patches. A list of near-optimum patches' names is introduced, and a variable that contains the length of this list is defined and used as a parameter in the whole code.

Commands that refer to the creation of the model's parts, the definition of datum points, axes and planes, as well as the necessary partitions of the model and the definitions of the parts' surfaces are formed fully parametrically, so that the model is smoothly created regardless of the inputs or the patch dimensions calculated by the first design part of the code. Similarly, for commands related to the implementation of several parts in their suitable positions in the assembly space, the definition of the datum points on the rigid bodies, the boundary conditions and the finite elements are constructed parametrically using the parts' dimensions and relative positions.

Input data includes an array of fiber direction angles for the patch. The code automatically calculates the number of plies based on this information and constructs loops that adapt to any number of plies.

A command set guarantees proper and automatic adjustments when the load direction is different from 0°. More specifically, the stepped cavity on the repaired plate and the patch in the assembly are suitably rotated and when determining the composite layup, each fiber direction angle is also rotated correspondingly.

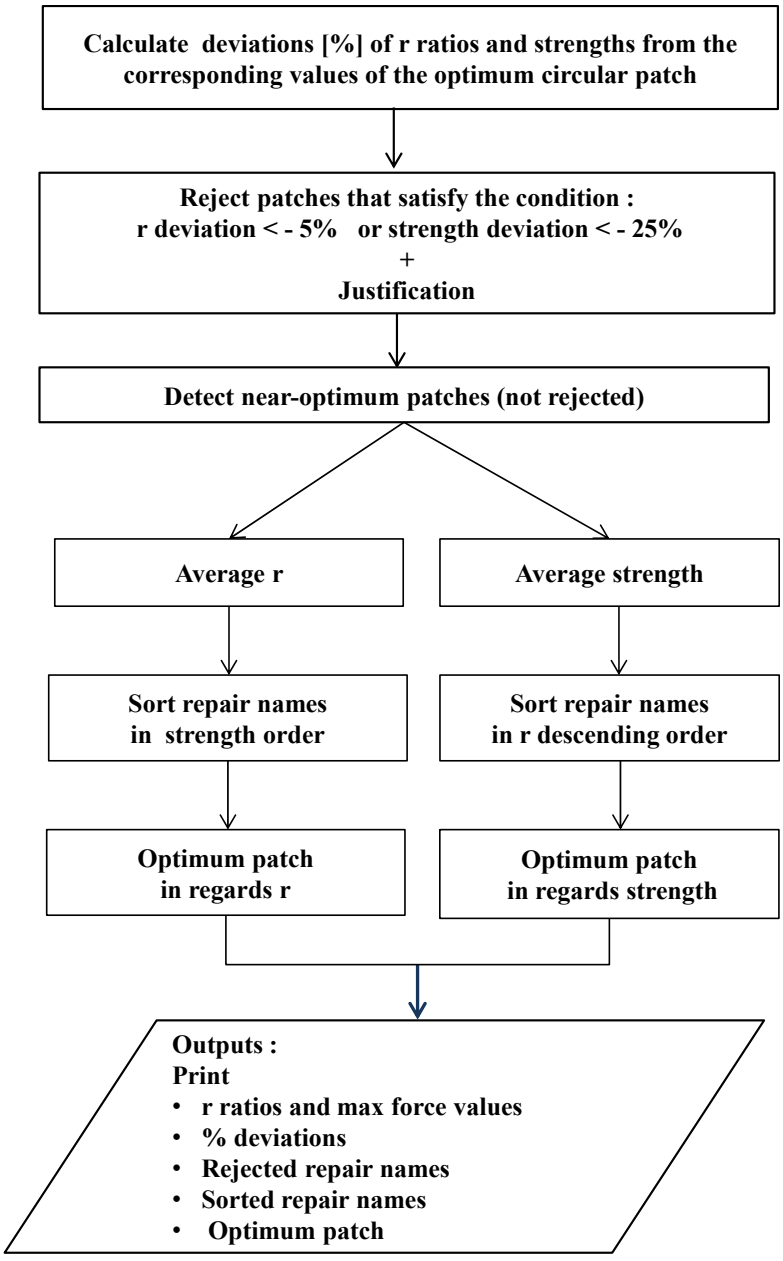

Figure 8. Detailed flowchart of the evaluation of the results and the assessment of the patches.

3. Results

In the present study, the designs that are listed in Table 5, whereby each patch name, as explained previously, represents the methods via which the patch's geometrical characteristics will be calculated, were investigated in comparison with a reference circular patch under compressive load. Then, the five best designs (Figure 9) were selected to be evaluated under tension and compression in three load directions, as follows: 0°, 45° and 90°. More specifically, five coded names of patches are introduced to the algorithm as inputs, namely Patch (I) for NR-XP-NC-AD, Patch (II) for NR-XYP-KT-G, Patch (III) for NR-XYP-KT-FD, Patch (IV) for NR-12L-MS-G and Patch (V) for NR-XYP-MS-G. An illustration of the algorithm outputs is shown in Figure 10, where on the top, the stresses of three different cases are presented, and on the bottom, the outputs of the algorithm that compare maximum forces, r ratios and deviations are presented.

Table 5. Patch designs that were evaluated in compression.

Specimen	Vmatloss [mm^3]	Difference from Circular [%]	r Ratio	Specimen	Vmatloss [mm^3]	Difference from Circular [%]	r Ratio
R-NL-C4-FD	569.17	−34.1	0.09	NR-NL-C5-FD	227.01	−23.9	0.25
R-NL-C5-FD	408.49	−39.5	0.11	NR-NL-C6-FD	177.79	−22.9	0.33
R-NL-C6-FD	314.23	−30.2	0.17	NR-NL-C7-FD	145.35	−19.9	0.42
R-NL-C7-FD	253.2	−44.9	0.16	NR-NL-C8-FD	122.5	−14.2	0.53
R-NL-C8-FD	210.85	−48.9	0.18	NR-NL-C9-FD	105.6	−32.9	0.48
R-NL-C9-FD	179.93	−44.9	0.23	NR-NL-C10-FD	96.62	−14.2	0.67
R-NL-C10-FD	156.46	−46.2	0.26	NR-XP-NC-AD	77.397	1.5	0.99
R-XP-NC-AD	215.12	−34.2	0.23	NR-XYP-NC-AD	255.82	−5.7	0.28
R-XYP-NC-AD	400.69	−26.0	0.14	NR-XYP-MS-G	250.5	−3.2	0.29
R-XYP-MS-G	389.47	−14.6	0.17	NR-XYP-MS-FD	144.49	−50.3	0.26
R-XYP-MS-FD	356.11	−29.0	0.15	NR-XYP-KT-G	1083	1.5	0.07
R-12L-NC-AD	1051	−25.1	0.05	NR-XYP-KT-FD	566.37	−2.3	0.13
R-12L-MS-G	1024.1	−22.5	0.06	NR-12L-NC-AD	456.62	−18.3	0.14
R-12L-MS-FD	1402.3	−5.2	0.05	NR-12L-MS-G	449.19	0.4	0.17
NR-NL-C2-FD	870.67	−22.0	0.07	NR-12L-MS-FD	364.5	−21.8	0.16
NR-NL-C4-FD	309.17	−21.8	0.19				

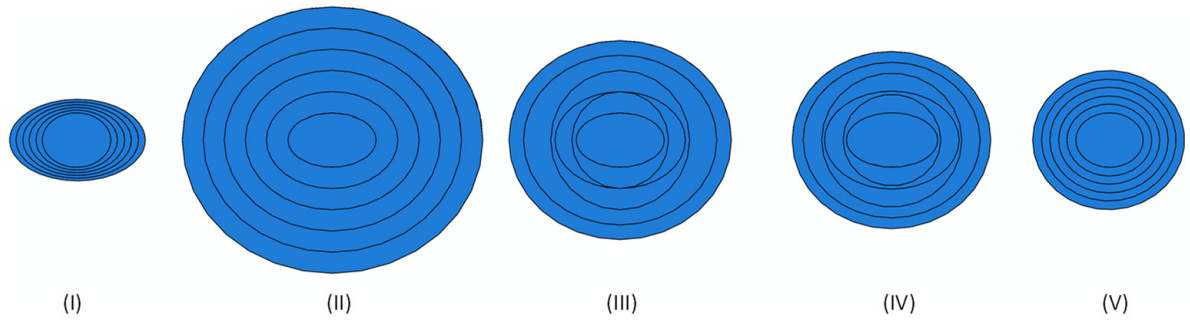

Figure 9. The five near-optimum elliptical patches that were designed and examined in the current study. The different geometries are numbered from (I) to (V).

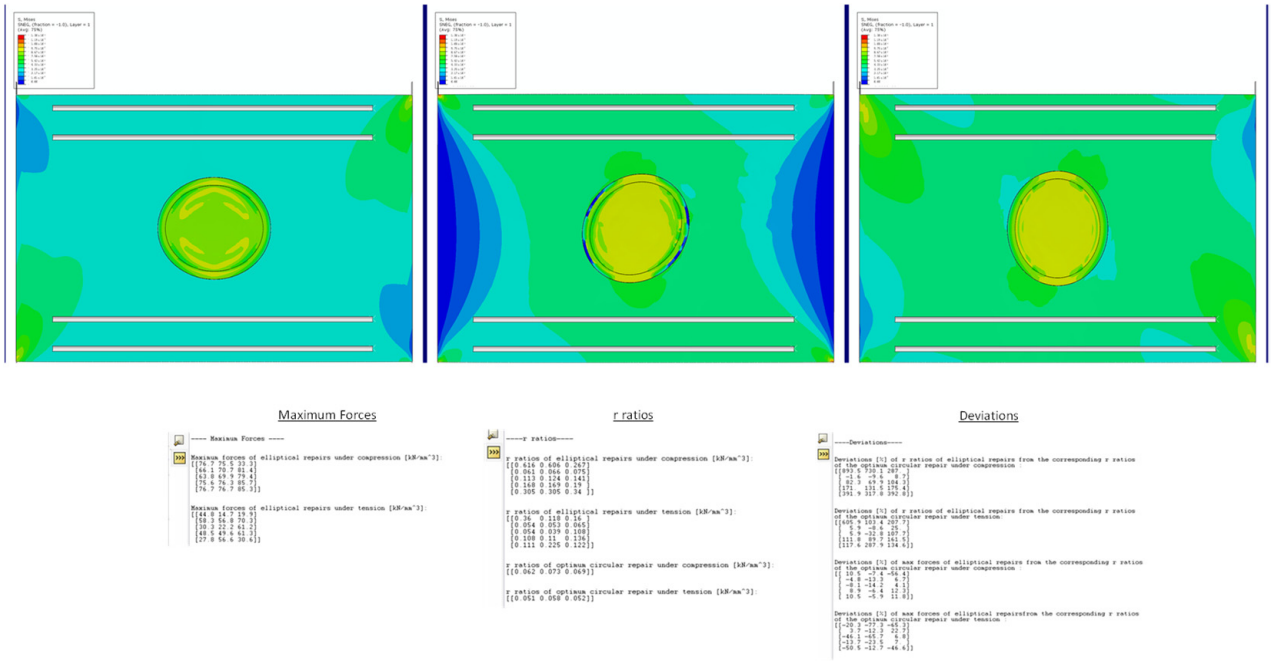

Figure 10. On the top, illustration of FE simulation for three different case; on the bottom, illustration of the post-processing code extracts of the analyses.

The results of the post-processing algorithm are presented in Figures 11 and 12. In compressive loading, at 0° and at 45°, patch (I) is deemed optimal, but it is insufficient for loading at 90° and is rejected. At 90°, patch (V) proves to be optimal, which for a load at 0° and 45°, held second place. The results are justified because patch (I) is designed with the requirement to withstand loading at 0° only. Consequently, the step length in the 0° direction is sufficient and the repair has a high strength, while the step in the 90° direction is too short and is insufficient for a smooth load transfer. That is, the small step length at 90° greatly reduces the patch volume and, therefore, the volume of removed healthy material in the repair and has a very high r ratio for loading at 0° and 45° (a 8935% and 730.1%, respectively, higher r ratio than the optimum circular). However, this costs the inadequacy of the patch for loading at 90° (a 56.4% lower strength than the optimal circular).

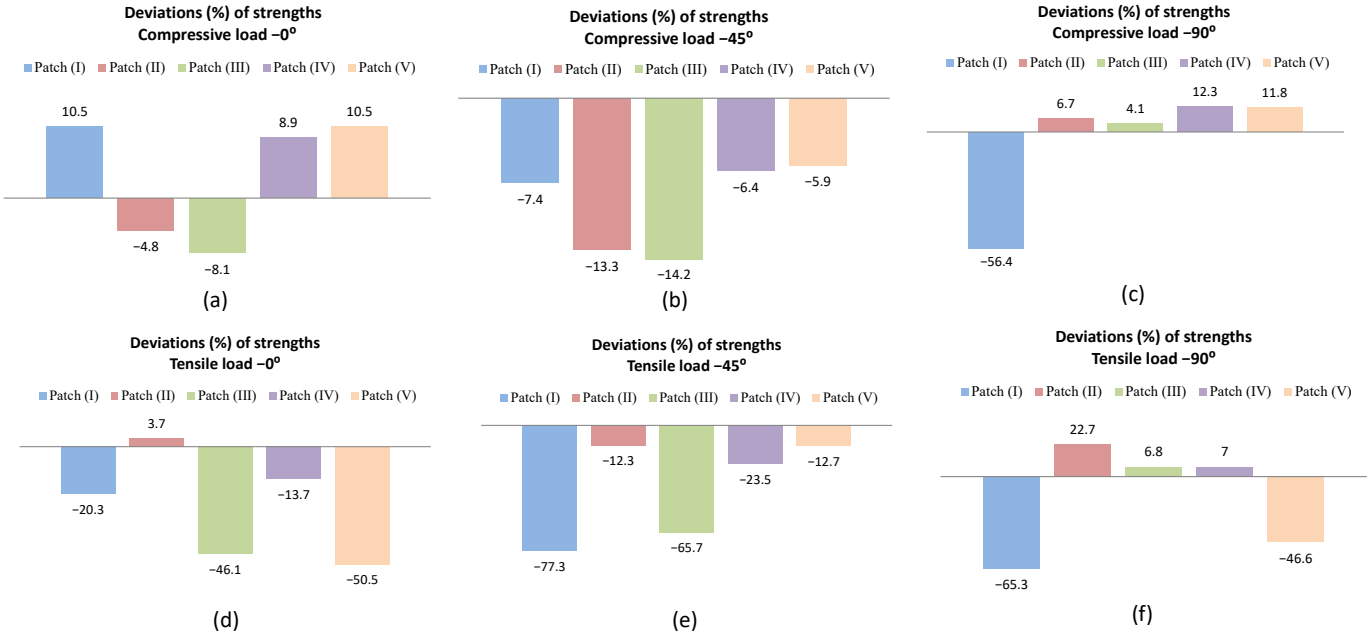

Figure 11. Results for the five near-optimum patches' deviation compared to the circular patch strength for compression (**a**–**c**) and tension (**d**–**f**).

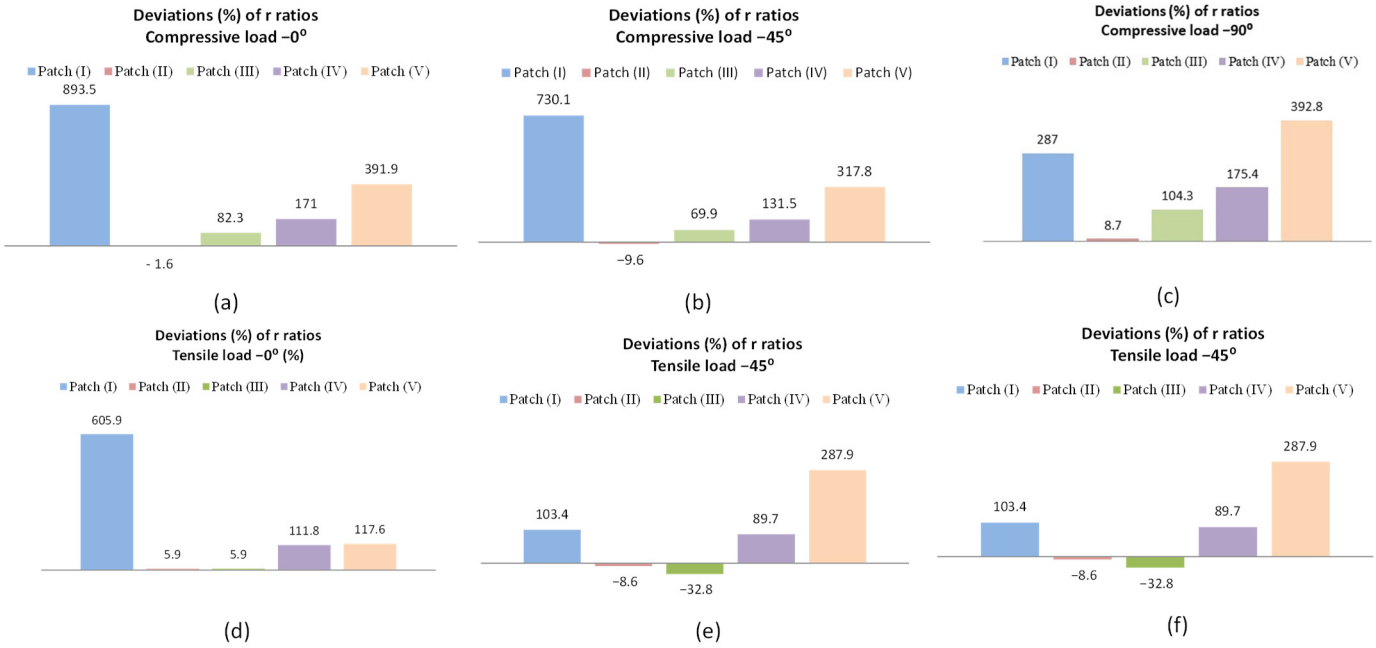

Figure 12. Results for the five near-optimum patches' deviation compared to the circular patch r ratio for compression (**a**–**c**) and tension (**d**–**f**).

Furthermore, patch (II) in all three cases is either rejected or performs worst. This particular patch has been designed taking into account the stress concentration factor, Kt. This method leads to patches of quite large size, resulting in a very low r ratio, without high strength, as can be seen from the models.

For tensile loading, the results appear to be more complex. At 0°, as expected, patch (I) is considered optimal, but at 45° and 90°, it is rejected. Furthermore, the performance of patch (II) is similar to its performance in compressive loading. For loading at 45° and 90°, patches (IV) and (V) look optimal for the design of which the maximum stress method has been applied to calculate the scarf angle and the simple geometric relationship to

calculate the step. Finally, it is worth noting that for all three addresses, patch (IV) shows a satisfactory performance and is not rejected.

Regarding compressive loading in all directions, patches (I) and (II) are rejected for the reasons mentioned previously. For the rest of the patches, the average value of the strength and the average value of the r ratio are calculated for all three loading directions. It can be said that the ranking of the pads in terms of average strength and average r ratio is the same, with pad (V) being judged optimal and pad (IV) taking second place. Under tensile loading, no pad appears to be adequate, except pad (V), which appeared to be quite satisfactory in compressive loading as well.

Finally, the patches are evaluated in terms of the case of every loading. The algorithm locates the patches that are rejected and displays in detail the r or strength values that made them rejectable. Among the patches examined in this work, only patch (4) is judged as an optimal candidate, according to the criteria given to the algorithm. Therefore, there is no ranking in terms of decreasing r ratio or decreasing strength, and finally, patch (4) is chosen as the overall optimum.

The experimental validation of the results is strongly recommended, so that the findings can be verified and the accuracy and reliability of the models and the design methods can be examined. For this reason, specimens repaired with patch (IV) and circular patches with the aid of a laser manipulator [18,23,24] are tested according to ASTM D7136-15/D7137-17 [26], as shown in Figure 13. According to the test, the specimens with patch (IV) handled 6.7% more compressive load than the ones repaired with circular patches, a difference close to the 8.9% that the optimization study suggests.

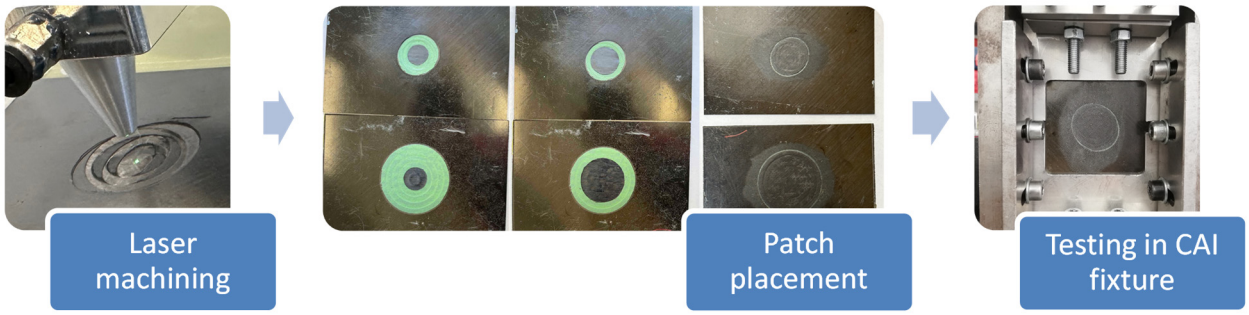

Figure 13. The repair patch procedure from patch creation to testing.

4. Discussion

The results from this study reveal that the elliptical form of repair patches can offer up to a 10.5% increase in strength and, at the same time, a 391.9% increase in r ratio (repair loaded at 0°) compared to the strength that the optimum circular patch provides. Also, an interesting conclusion that agrees with the results in the literature is the fact that the length of step plays an important role in the repair's efficiency, since repair (I) that does not have an adequate step length in the y direction exhibited a much lower strength than the circular patch (7.4% and 56.4% lower when loaded at 45° and 90°, respectively).

In conclusion, the goal of the study was achieved to a great extent, as the developed algorithm remarkably facilitated the modeling and examination of various designs for composite repair patches. The code can serve as a valuable tool and a foundation for future research and for the purpose of expanding the existing repair patch optimization methodologies.

The findings obviously highlight the crucial role of the step length in the loading direction, which significantly affects the repair's strength. As the scarf angle decreases (i.e., the step increases), the strength tends to increase significantly, but the r ratio decreases due to increased volume, which is consistent with the literature observation.

Furthermore, the optimum patches resulting from the proposed methods are much more efficient than the optimum circular patch. Specifically, patch III (NR-NS-5-9-G) offered a 10.7% higher strength and a 509.7% higher r ratio than the optimum circular patch.

Similarly, patch IV (NR-12L-MS-G) provided an 8.9% higher strength and a 171% higher r ratio. Thus, the adapted algorithmic design method for candidate optimum patches seems promising and if it was applied to more patch geometries and more loading conditions, it is hoped to offer very good approaches for determining the optimum repair patch. Finally, it can be said that optimum patch designs can reduce the machining times and can also lead to more accurate and efficient repairs.

Author Contributions: Conceptualization, S.P. and V.K.; methodology, M.-P.G. and S.P.; software, M.-P.G.; validation, S.P.; formal analysis, M.-P.G. and S.P.; investigation, M.-P.G. and S.P.; resources, V.K.; data curation, M.-P.G. and S.P; writing—original draft preparation, M.-P.G. and S.P.; writing—review and editing, S.P. and V.K.; visualization, S.P. and V.K.; supervision, S.P. and V.K.; project administration, V.K. All authors have read and agreed to the published version of the manuscript.

Funding: This research received no external funding.

Data Availability Statement: The data presented in this study are available on request from the corresponding author.

Conflicts of Interest: The authors declare no conflicts of interest.

References

1. Federal-Aviation-Administration. *Order 8900.1A—Flight Standards Information Management System*; Federal-Aviation-Administration: Washington, DC, USA, 2022.
2. Wu, C.; Chen, C.; He, L.; Yan, W. Comparison on damage tolerance of scarf and stepped-lap bonded composite joints under quasi-static loading. *Compos. Part B Eng.* **2018**, *155*, 19–30. [CrossRef]
3. Pierce, R.S.; Falzon, B.G. Modelling the size and strength benefits of optimised step/scarf joints and repairs in composite structures. *Compos. Part B Eng.* **2019**, *173*, 107020. [CrossRef]
4. Niedernhuber, M.; Holtmannspötter, J.; Ehrlich, I. Fiber-oriented repair geometries for composite materials. *Compos. Part B Eng.* **2016**, *94*, 327–337. [CrossRef]
5. Bendemra, H.; Compston, P.; Crothers, P.J. Optimisation study of tapered scarf and stepped-lap joints in composite repair patches. *Compos. Struct.* **2015**, *130*, 1–8. [CrossRef]
6. Wang, C.H.; Venugopal, V.; Peng, L. Stepped Flush Repairs for Primary Composite Structures. *J. Adhes.* **2015**, *91*, 95–112. [CrossRef]
7. Chamorro-Cruz, I.; López-Santiago, R.; Vázquez-Castillo, V.; Hernández-Moreno, H.; Beltrán-Zúñiga, M.A.; González-Velázquez, J.L.; Rivas-López, D.I. Elliptical one-side composite bonded repair analysis through a differential evolution algorithm. *Aircr. Eng. Aerosp. Technol.* **2023**, *95*, 1116–1127. [CrossRef]
8. Echer, L.; Souza CE, D.; Marczak, R.J. A Study on the Best Conventional Shapes for Composite Repair Patches. *Mater. Res.* **2021**, *24* (Suppl. S2), e20210304. [CrossRef]
9. Benyahia, F.; Albedah, A.; Bouiadjra, B.A.B. Elliptical and circular bonded composite repair under mechanical and thermal loading in aircraft structures. *Mater. Res.* **2014**, *17*, 1219–1225. [CrossRef]
10. Collombet, F.; Davila, Y.; Avila, S.; Morales, A.; Crouzeix, L.; Grunevald, Y.-H.; Hernandez, H.; Rocher, N.; Cénac, F. Proof of a composite repair concept for aeronautical structures: A simplified method. *Mech. Ind.* **2019**, *20*, 812. [CrossRef]
11. Tashi, S.; Abedian, A. A comprehensive 2 Dimensional and 3 Dimensional FEM study of scarf repair for a variety of common composite laminates under in-plane uniaxial and equibiaxial loadings. *Int. J. Adhes. Adhes.* **2022**, *114*, 103092. [CrossRef]
12. Wang, C.; Gunnion, A. Optimum shapes of scarf repairs. *Compos. Part A Appl. Sci. Manuf.* **2009**, *40*, 1407–1418. [CrossRef]
13. Hall, Z.E.C.; Liu, J.; Brooks, R.A.; Liu, H.; Crocker, J.W.M.; Joesbury, A.M.; Harper, L.T.; Blackman, B.R.K.; Kinloch, A.J.; Dear, J.P. The effectiveness of patch repairs to restore the impact properties of carbon-fibre reinforced-plastic composites. *Eng. Fract. Mech.* **2022**, *270*, 108570. [CrossRef]
14. Wang, C.H.; Gunnion, A.J. Optimum shapes for minimising bond stress in scarf repairs. *Aust. J. Mech. Eng.* **2008**, *6*, 153–158. [CrossRef]
15. Ramji, M.; Srilakshmi, R.; Prakash, M. Towards optimization of patch shape on the performance of bonded composite repair using FEM. *Compos. Part B Eng.* **2013**, *45*, 710–720. [CrossRef]
16. Wang, C.; Duong, C. Design and optimization of scarf repairs. In *Bonded Joints and Repairs to Composite Airframe Structures*; Academic Press: London, UK, 2016; ISBN 9780124171534. [CrossRef]
17. Pitanga, M.Y.; Cioffi, M.O.H.; Voorwald, H.J.C.; Wang, C.H. Reducing repair dimension with variable scarf angles. *Int. J. Adhes. Adhes.* **2021**, *104*, 102752. [CrossRef]
18. Psarras, S.; Loutas, T.; Papanaoum, M.; Triantopoulos, O.K.; Kostopoulos, V. Investigating the Effect of Stepped Scarf Repair Ratio in Repaired CFRP Laminates under Compressive Loading. *J. Compos. Sci.* **2020**, *4*, 153. [CrossRef]
19. Barbosa, N.G.C.; Campilho, R.D.S.G.; Silva, F.J.G.; Moreira, R.D.F. Comparison of different adhesively-bonded joint types for mechanical structures. *Appl. Adhes. Sci.* **2018**, *6*, 15. [CrossRef]

20. Damghani, M.; Bolanos, S.; Chahar, A.; Matthews, J.; Atkinson, G.A.; Murphy, A.; Edwards, T. Design, novel quality check and experimental test of an original variable length stepped scarf repair scheme. *Compos. Part B Eng.* **2022**, *230*, 109542. [CrossRef]
21. Yoo, J.-S.; Truong, V.-H.; Park, M.-Y.; Choi, J.-H.; Kweon, J.-H. Parametric study on static and fatigue strength recovery of scarf-patch-repaired composite laminates. *Compos. Struct.* **2016**, *140*, 417–432. [CrossRef]
22. Bhise, V.; Kashfuddoja, M.; Ramji, M. Optimization of circular composite patch reinforcement on damaged carbon fiber reinforced polymer laminate involving both mechanics-based and genetic algorithm in conjunction with 3D finite element analysis. *J. Compos. Mater.* **2013**, *48*, 2679–2695. [CrossRef]
23. Psarras, S.; Loutas, T.; Galanopoulos, G.; Karamadoukis, G.; Sotiriadis, G.; Kostopoulos, V. Evaluating experimentally and numerically different scarf-repair methodologies of composite structures. *Int. J. Adhes. Adhes.* **2019**, *97*, 102495. [CrossRef]
24. Psarras, S.; Loutas, T.; Sotiriadis, G.; Kostopoulos, V. Evaluating the compressive strength of stepped scarf repaired single stiffener composite panels. *J. Compos. Mater.* **2023**, *57*, 2887–2898. [CrossRef]
25. *AITM 1-0010*; Airbus Test Method. Determination of Compression Strength After Impact. Airbus S.A.S Engineering Directorate: Blagnac, France, 2005.
26. *ASTM. D7137/D7137M—07*; Standard Test Method for Compressive Residual Strength Properties of Damaged Polymer Matrix Composite Plates. ASTM: West Conshohocken, PA, USA, 2011; p. 16. [CrossRef]